doi:10.1016/j.jmb.2009.05.018 J. Mol. Biol. (2009) 390, 17–25

JMB

Available online at www.sciencedirect.com

ScienceDirect

ELSEVIER

COMMUNICATION

Structural and Functional Model for Ionic (K^+/Na^+) and pH Dependence of GTPase Activity and Polymerization of FtsZ, the Prokaryotic Ortholog of Tubulin

Jesús Mendieta[1,2], Ana Isabel Rico[3], Eduardo López-Viñas[1,4], Miguel Vicente[3], Jesús Mingorance[5]† and Paulino Gómez-Puertas[1]*†

[1]*Centro de Biología Molecular "Severo Ochoa" (CSIC-UAM), Campus de Cantoblanco, c/Nicolás Cabrera, 1, 28049 Madrid, Spain*

[2]*Biomol-Informatics SL, Parque Científico de Madrid, Campus de Cantoblanco, c/Einstein, 13, 28049 Madrid, Spain*

[3]*Consejo Superior de Investigaciones Científicas, Centro Nacional de Biotecnología (CNB-CSIC), Campus de Cantoblanco, c/Darwin, 3, 28049 Madrid, Spain*

[4]*CIBER "Fisiopatología de la Obesidad y la Nutrición" (CB06/03), Instituto de Salud Carlos III, 28029, Madrid, Spain*

[5]*Servicio de Microbiología y Unidad de Investigación, Hospital Universitario La Paz, Paseo de la Castellana, 261, 28046 Madrid, Spain*

Received 9 February 2009; received in revised form 28 April 2009; accepted 12 May 2009
Available online 15 May 2009

Edited by D. Case

Bacterial cell division occurs through the formation of a protein ring (division ring) at the site of division, with FtsZ being its main component in most bacteria. FtsZ is the prokaryotic ortholog of eukaryotic tubulin; it shares GTPase activity properties and the ability to polymerize *in vitro*. To study the mechanism of action of FtsZ, we used molecular dynamics simulations of the behavior of the FtsZ dimer in the presence of GTP–Mg^{2+} and monovalent cations. The presence of a K^+ ion at the GTP binding site allows the positioning of one water molecule that interacts with catalytic residues Asp235 and Asp238, which are also involved in the coordination sphere of K^+. This arrangement might favor dimer stability and GTP hydrolysis. Contrary to this, Na^+ destabilizes the dimer and does not allow the positioning of the catalytic water molecule. Protonation of the GTP gamma-phosphate, simulating low pH, excludes both monovalent cations and the catalytic water molecule from the GTP binding site and stabilizes the dimer. These molecular dynamics predictions were contrasted experimentally by analyzing the GTPase and polymerization activities of purified *Methanococcus jannaschii* and *Escherichia coli* FtsZ proteins *in vitro*.

Keywords: FtsZ; molecular dynamics; GTPase; polymerization; monovalent cations

*Corresponding author. E-mail address: pagomez@cbm.uam.es.

† J.M. and P.G.-P. are the co-last authors.

Abbreviations used: MD, molecular dynamics; $FtsZ_{EC}$, *Escherichia coli* FtsZ; $FtsZ_{MJ}$, *Methanococcus jannaschii* FtsZ.

FtsZ is the central protein of the prokaryotic cell division machinery. It is the most abundant among all known essential division proteins, the first to localize to the division site, together with FtsA and ZipA,[1,2] and the most conserved throughout the bacterial and archaeal domains.[3–5] FtsZ localizes to

the cell center prior to division and forms a protein ring, the Z-ring, beneath the inner cell membrane.[6] Rings formed by several FtsZ filaments, 5 nm in diameter and spaced an average of 9.3 nm apart, have been observed *in vitro*.[7,8] In addition to the central role that it plays in division as an organizer for the rest of the division complexes, it has been suggested that the Z-ring itself has an active motor function during cytokinesis.[9] Force-generating mechanisms have been previously proposed based on the structural or physical properties of FtsZ filaments,[10–12] but specific molecular explanation is lacking.

Sequence and structural comparisons of FtsZ with eukaryotic tubulin indicate that the two proteins are homologous.[3,13] As tubulin, FtsZ binds GTP and GDP *in vitro*, has GTPase activity, and polymerizes in a GTP-dependent manner.[3,13] Nucleotide binding is independent of any other factor, but the catalytic and polymerization activities depend on the presence of divalent and monovalent cations.[14–16] The physiological divalent cation is Mg^{2+}, which is bound to the phosphates of the nucleotide, and it has been implicated in oligomerization.[17]

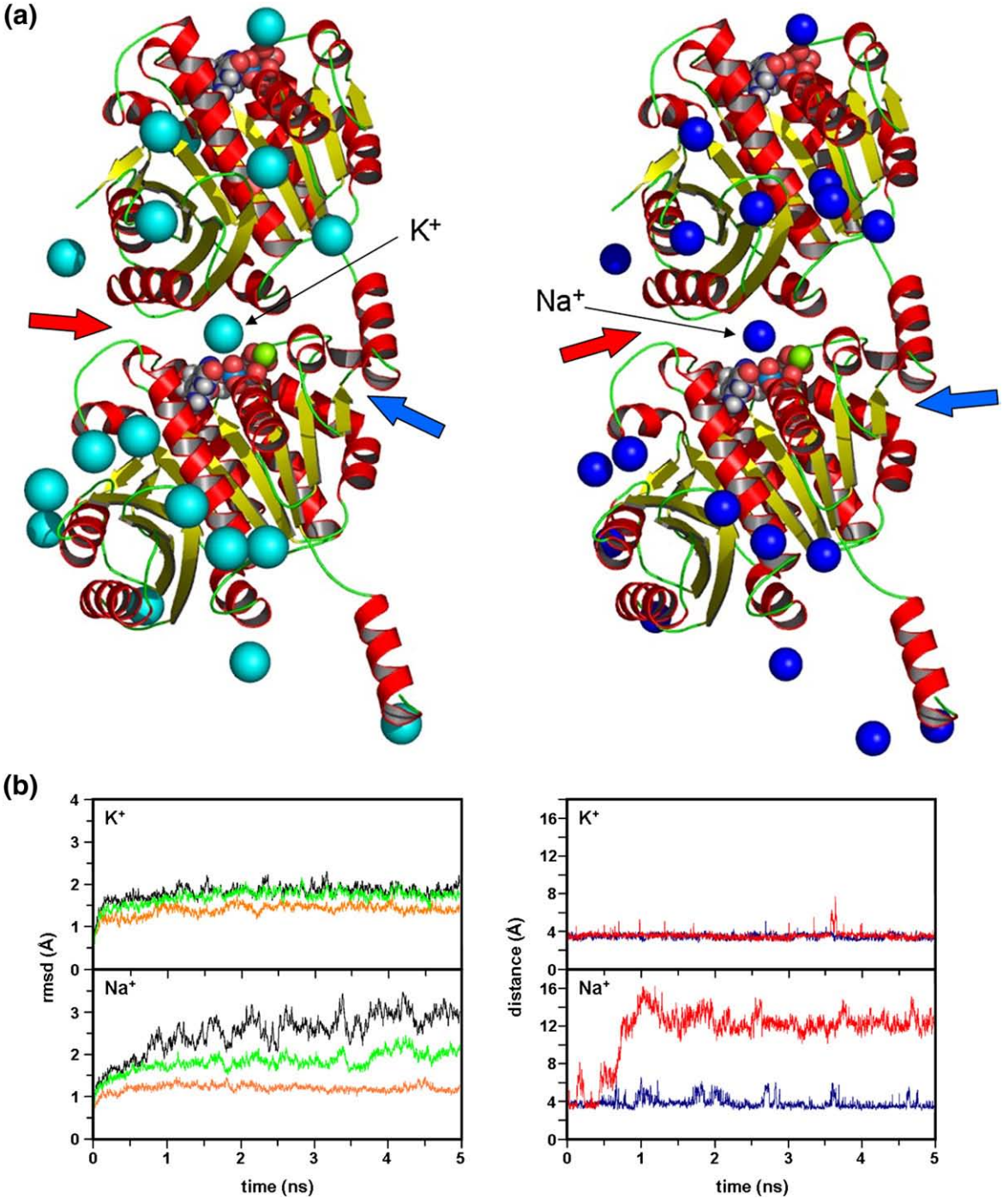

Fig. 1 *(legend on next page)*

In the case of FtsZ, the role of the monovalent cation is not known. The binding affinity is very low, in the millimolar range, and the cation itself has not been detected in crystallographic structures experimentally obtained in the presence of lithium salts and in the absence of Na^+ or K^+. There are some differences between bacterial species with regard to the cation preference, so while FtsZ from *Azotobacter vinelandii* and that from *Thermotoga maritima* are activated by Na^+ and K^+, FtsZ from *Escherichia coli* ($FtsZ_{EC}$) shows some preference for K^+ at neutral pH but may be activated by Na^+ at low pH (6.0–6.5) or high protein concentration.[18] In *Methanococcus jannaschii*, FtsZ activity depends exclusively on the presence of K^+; it is not measurable for any Na^+ concentration at neutral pH.[19] In $FtsZ_{EC}$, cation binding is linked to polymerization, whereby the uptake of one ion is associated with the incorporation of one monomer into the growing polymer.[16]

Biochemical studies and macromolecular structures of several proteins bound to K^+ or Na^+ at the active sites show a significant role for monovalent cations in the activity of a broad range of enzymes.[20–22] It is not known what physiological role the activation of FtsZ by the monovalent cation might have. In spite of the low binding affinity, the intracellular concentration of K^+ is probably always high enough to saturate FtsZ in growing cells (0.1–0.5 M)[16] and K^+ therefore cannot temporally or spatially control FtsZ polymerization. It has rather been proposed that K^+ provides a weak interaction between monomers that might be important in determining the highly dynamic behavior of FtsZ polymers.[16]

In this work, we studied the role of monovalent cations in FtsZ activity by means of molecular dynamics (MD) and corroborated the *in silico* results by measuring GTPase activity and polymerization.

Modeling structural stability of FtsZ dimer in the presence of K^+ or Na^+

We aimed to explain the differential behavior of FtsZ in the presence of Na^+ or K^+[16,19] and used MD techniques to simulate the effect of these ions on the FtsZ dimer structure. We used the crystallized form of the *M. jannaschii* FtsZ ($FtsZ_{MJ}$) dimer[23] as a base. We hoped to perform additional simulations with the $FtsZ_{EC}$ dimer, but no crystal structure has yet been obtained for this protein and the quality of homology models of the $FtsZ_{EC}$ dimer is too poor for them to be used in MD. We performed computational simulation using the structure of $FtsZ_{MJ}$ and *in vitro* analysis of the GTPase and polymerization activities of $FtsZ_{MJ}$ and $FtsZ_{EC}$.

The crystal structure of $FtsZ_{MJ}$ (Protein Data Bank entry 1W5A)[23] was subjected to initial equilibration before starting MD simulation using the AMBER suite.[24] Two conditions, by adding either K^+ or Na^+, were used in a coulombic potential grid to ensure the electrical neutrality of the system. Figure 1a shows the positioning of the Na^+ or K^+ atoms in the solvent boxes around the $FtsZ_{MJ}$ dimer after equilibration. In both cases, an atom of the monovalent cation was found in the interface between the two protein monomers (Fig. 1a, black arrows), close to the GTP binding site. This is likely a consequence of the negative charge of GTP. Next, a 5-ns MD simulation was performed, and changes in the structure of FtsZ were followed by measuring root-mean-square deviation (RMSD) values of the whole protein dimer and of each monomer with respect to the initial position in the crystal. To measure changes in dimer arrangement, we continuously annotated the distances between selected pairs of amino acids located at the interface between monomers. Those pairs of residues correspond to two of the three protein–protein contacts described in the original report of the $FtsZ_{MJ}$ dimer structure:[23] the C^α–C^α distance between Asp26 (upper monomer) and Lys80 (lower monomer), positioned in the area of the H0 helix contact (blue arrows in Fig. 1a), and the C^α–C^α distance between Glu302 (upper monomer) and Lys205 (lower monomer), located in the opposite position of the interface between monomers (red arrows in Fig. 1a). Continuous measurements of the RMSD and selected distances are shown in Fig. 1b. No significant protein

Fig. 1. MD analysis of FtsZ dimer stability in the presence of K^+ or Na^+. MD simulations were performed using the SANDER module of the AMBER9 package.[24] Initial conditions were established using the crystallized structure of the $FtsZ_{MJ}$ dimer (Protein Data Bank code 1W5A[23]) surrounded by a solvent box created with a minimum distance of 12 Å from the edge and the closest atom of the solute. Na^+ or K^+ ions were added to neutralize the whole system. Adaptation of the system to the AMBER force field was performed by 10,000 steps of energy minimization using a cutoff of 10.0 Å. During the initial heating phase (200 ps), temperature was raised from 0 to 298 K, restraining the position of C^α atoms in the solute with a force constant of 20 kcal·mol^{-1}. In a second phase, the force constant was reduced stepwise. After equilibration, 5 ns of unrestrained MD was performed in each case. The SHAKE algorithm was applied to constrain bonds involving hydrogen atoms to their equilibrium values. The list of non-bonded pairs was updated every 25 steps, and coordinates were saved every 2 ps. Periodic boundary conditions were applied and electrostatic interactions were represented using the smooth particle mesh Ewald methods with a grid spacing of ~1 Å. (a) Cartoon representation of the FtsZ dimer showing the positioning of K^+ (left) or Na^+ (right) ions placed in a shell around the system using a coulombic potential in a grid of 1 Å as implemented in the XLEaP module of AMBER9. Black arrows indicate the presence of an atom of K^+ or Na^+ in the GTP site of the FtsZ dimer. Blue and red arrows point to the measured contacts between the two monomers (E302–K205 and D26–K80, respectively). (b) Left: RMSD values measured for the whole dimer (black), lower monomer (orange), and upper monomer (green) during a 5-ns MD trajectory in the presence of K^+ (top panel) or Na^+ (bottom panel) cations. Right: continuous measuring of C^α–C^α distances between residues E302–K205 (blue) and D26–K80 (red) during a 5-ns MD trajectory in the presence of K^+ (top panel) or Na^+ (bottom panel). Distortion of the FtsZ dimer in the presence of Na^+ is patent in both RMSD and C^α–C^α measurements (see the text).

movement was observed during the MD trajectory when K^+ was used as the counterion, indicating that the contacts between domains remained unchanged, with an average global RMSD of the upper monomer of 1.88±0.11 Å in the last 2 ns of the simulation. However, in the presence of Na^+, the RMSD value for the displacement of the upper monomer with respect to the lower one increased to 2.87±0.24 Å on average in the last 2 ns and the distance between Glu302 and Lys205 increased from 4 to 13 Å. These indicate the rupture of the selected contact. Relevant intradomain movements were not observed in either

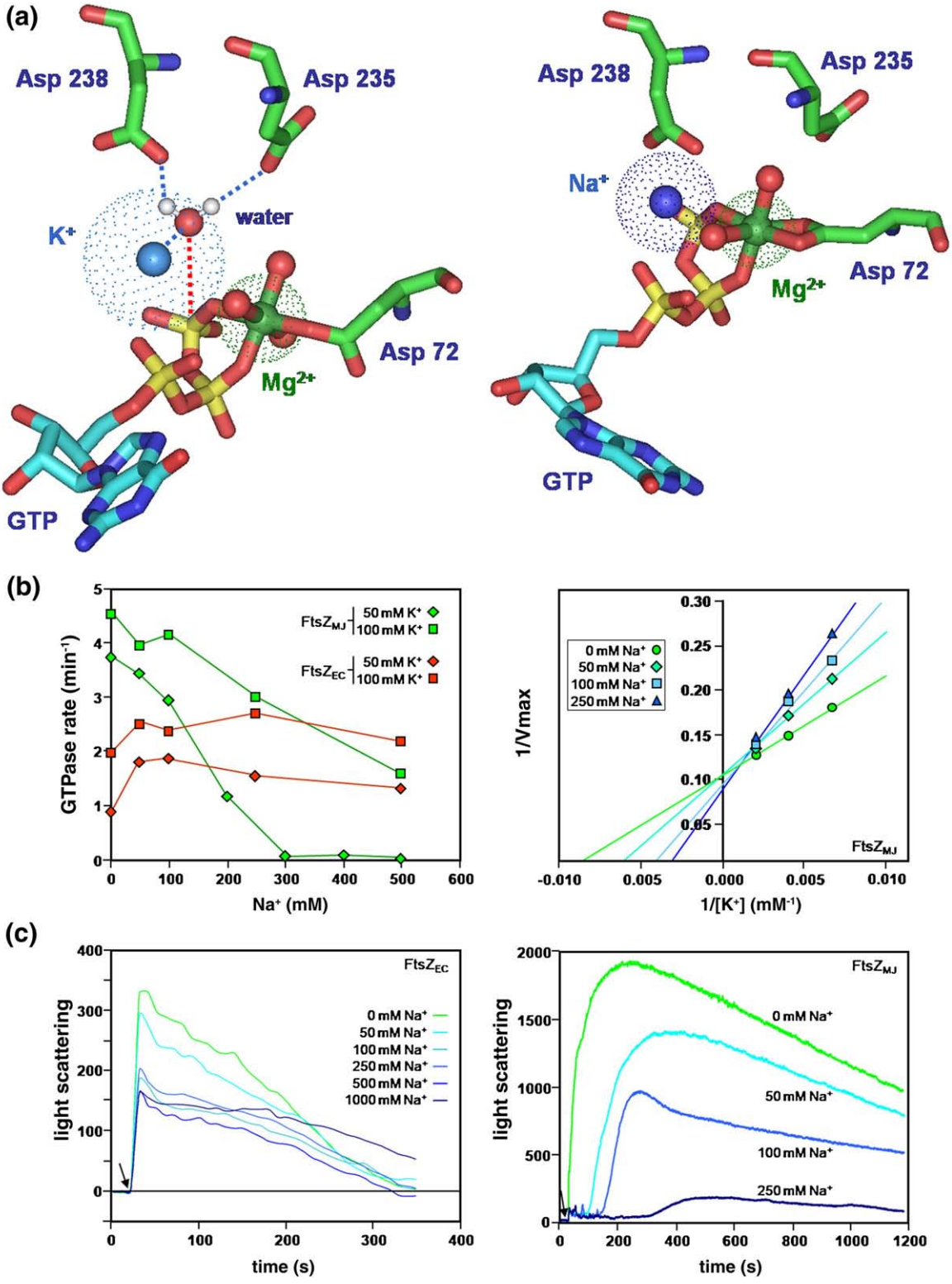

Fig. 2 *(legend on next page)*

case, nor were changes in the relative position of GTP and Mg^{2+} with respect to the contact residues in the lower monomer of FtsZ.

GTP binding site and GTPase activity

Our results suggest some important changes in the dimer interface between the presence of K^+ and that of Na^+. Figure 2a shows the structure of the catalytic site of the two dimers after 5 ns of MD simulation in detail. In the presence of K^+, the GTP binding site has a water molecule located in a position compatible with the attack distance of the γ-phosphorus of GTP. This water molecule is in the coordination sphere of the K^+ ion (the distance between the K^+ and the water oxygen is 3 Å), and at the same time it is in contact with the catalytic residues Asp235 and Asp238 of the upper monomer. However, in the presence of Na^+ (Fig. 2a, right), the smaller coordination sphere of this cation does not allow the positioning of a water molecule in the vicinity (including the original water molecules located in the active site in the crystal structure); its position is occupied by oxygen atoms from the Asp238 residue and a phosphate group. Here, the absence of the water molecule necessary to hydrolyze the GTP must result in the absence of GTPase activity in the dimer.

Thus, we propose that K^+ might activate the GTPase activity of FtsZ, but Na^+ cannot. As both Na^+ and K^+ are bound to the same site in the dimer structure, our results also suggest that Na^+ might be a competitive inhibitor of K^+ for the GTPase activity of FtsZ.

In addition, although both ions retain the capacity to connect the two protein monomers via the GTP molecule and maintain the dimerized structure, the final positionings of bridging residues are different (Figs. 1b and 2a). This affects their polymerization properties.

To test this hypothesis, we calculated the GTPase activities of purified $FtsZ_{MJ}$ and $FtsZ_{EC}$ in the presence of different concentrations of K^+ and Na^+. As shown in Fig. 2b, Na^+ is a competitive inhibitor of K^+ for $FtsZ_{MJ}$, as predicted by the MD model. In contrast, Na^+ did not compete with K^+ in $FtsZ_{EC}$, most likely due to differences in the affinities for the two cations in this system.[16] It should be noted that the MD simulation was done only for $FtsZ_{MJ}$, as there is no structure of $FtsZ_{EC}$ available.

Correspondence between GTPase activity at different concentrations of Na^+ and the capacity of FtsZ to polymerize was analyzed by light scattering (Fig. 2c). In agreement with the corresponding GTPase activity and MD simulation results discussed above, $FtsZ_{MJ}$ polymerization was almost completely inhibited when the Na^+ concentration was increased from 0 to 250 mM (Fig. 2c, right) even at a high K^+ concentration (500 mM). This confirms the role of Na^+ as a competitive inhibitor of this process. $FtsZ_{EC}$ polymerization at a K^+ concentration of 150 mM (Fig. 2c, left) was also partially inhibited when Na^+ concentration was increased from 0 to 100 mM, but in agreement with the results obtained for GTPase activity, polymer formation cannot be completely inhibited by further increases in Na^+ concentration, even to 1 M.

Effect of pH on GTPase activity and polymerization of FtsZ

Different reports indicate that $FtsZ_{EC}$ GTPase activity decreases at pH values lower than 6.8, but it retains its capacity to polymerize even in the absence of K^+.[13,14,18,19] To study the apparent contradiction between GTPase activity and polymerization capabilities, we have compared results obtained from MD and those obtained from biochemical techniques. MD simulations of low pH conditions can be done by protonation of histidine residues and GTP, as pK_a values of both molecules are in the same range, around 6.8.[27] As there are no histidine residues located in the vicinity of the active site of FtsZ, and they are not involved in essential interactions for maintaining the FtsZ dimer structure, acidic conditions were established only by

Fig. 2. Differential GTPase activity and polymerization of FtsZ in the presence of K^+ or Na^+. (a) Schematic representation of the active site for the $FtsZ_{MJ}$ dimer after a 5 -ns MD simulation in the presence of K^+ (left) and Na^+ (right). Residues directly involved in GTP hydrolysis from lower (Asp72) and upper (Asp235, Asp238) FtsZ monomers are depicted. The presence of a water molecule in the appropriate position for catalysis of the GTP molecule, only in the presence of K^+ (not of Na^+), is indicated. (b) Left: The effect on $FtsZ_{MJ}$ and $FtsZ_{EC}$ GTPase activities of increasing the concentration of Na^+ in the presence of different concentrations of K^+. Right: Double reciprocal plot of $FtsZ_{MJ}$ GTPase activity at increasing concentration of K^+ in the presence of different concentrations of Na^+. $FtsZ_{EC}$ was purified by the Ca^{2+}-induced precipitation method.[17] $FtsZ_{MJ}$ was purified in a Ni^{2+}-affinity column.[25] Proteins were stored at −80 °C and, prior to use, $FtsZ_{MJ}$ was further purified by a heat shock (15 min at 65 °C) followed by centrifugation, and both $FtsZ_{MJ}$ and $FtsZ_{EC}$ proteins were desalted by exchanging the storage buffer with TM buffer ($FtsZ_{MJ}$: 50 mM Tris, pH 6.5, and 10 mM $MgCl_2$; $FtsZ_{EC}$: 50 mM Tris, pH 7.5, and 10 mM $MgCl_2$) in a 5-ml Hi-Trap™ desalting column (Pharmacia Biotech). To test polymerization in the absence of Na^+, we detected the GTPase activity either by thin-layer chromatography[13] or by a colorimetric assay[26] using 10 μM FtsZ and GTP (Tris salt; G9002, Sigma) as substrate. Activity values were calculated by measuring the slope of the linear part of the enzymatic kinetics (eight measurements done in triplicate for each experiment) in the presence of GTP. (c) Light-scattering analysis of the assembly of purified $FtsZ_{EC}$ (left) and $FtsZ_{MJ}$ (right) at different concentrations of Na^+ in the presence of 150 mM K^+ for $FtsZ_{EC}$ or 500 mM K^+ for $FtsZ_{MJ}$. Polymerization was followed by 90° light scattering in a Hitachi F-2500 fluorescence spectrophotometer at excitation and emission wavelengths of 350 nm. The light-scattering signal was corrected for background signal obtained before the addition of GTP or with GTP in the absence of monovalent salts. All the assays were performed at 25 °C and pH 7.5 for $FtsZ_{EC}$ and at 55 °C and pH 6.5 for $FtsZ_{MJ}$. The arrow indicates the point at which GTP (final concentration of 0.5 mM) was added.

protonation of the gamma-phosphate of GTP prior to MD equilibration. The first consequence of GTP protonation was the absence of the positive monovalent cation (both Na^+ and K^+) in the dimer interface during equilibration. This was probably due to the lower negative charge compared with unprotonated GTP (Fig. 3).

After equilibration, a 5-ns MD simulation was performed to measure the stability of the dimerized structure. As shown in Fig. 3b, global RMSD values did not fluctuate over values higher than 2 Å and the distances measured between selected residues located in the interface did not increase significantly. These indicate that the whole dimer remained stable. In addition, during the simulation, no water molecule was found at a distance compatible for the necessary attack that leads to GTP hydrolysis (Fig. 3a), so GTPase activity was concluded to be inhibited. In summary, the simulated conditions for the FtsZ dimer interface at low pH showed the absence of GTPase activity and the stabilization of the dimer in the protonated FtsZ structure. Then, it is predicted that a simultaneous decrease of GTPase activity is parallel with a decrease in pH and the presence of stable polymers at all acidic pHs, independently of the GTPase activity.

To test this hypothesis, we measured the GTPase activities of $FtsZ_{MJ}$ and $FtsZ_{EC}$ *in vitro* over a wide

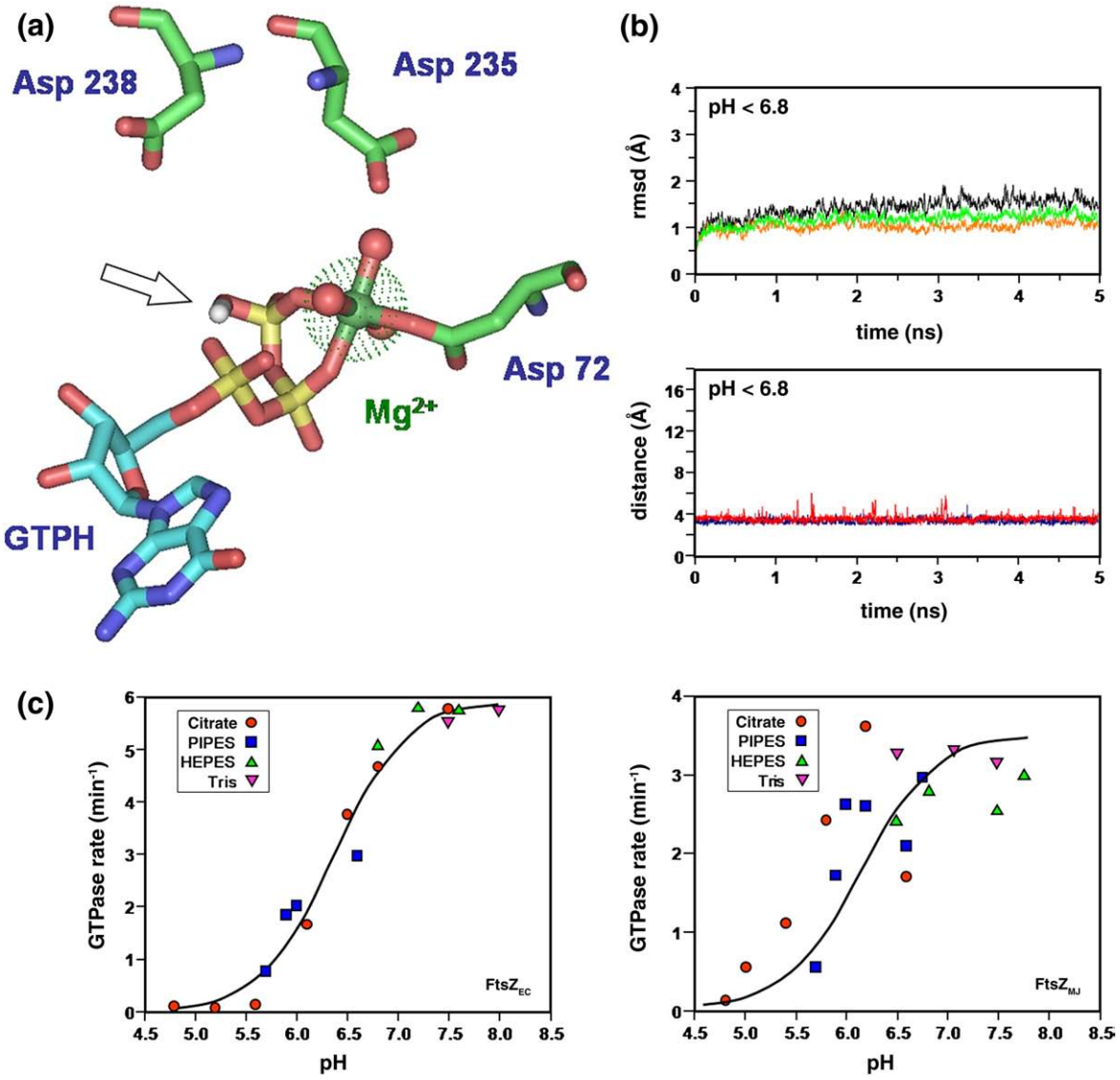

Fig. 3. Effect of pH on FtsZ dimerization and GTPase activity. (a) Active site for $FtsZ_{MJ}$ after 5 ns of MD simulation in the presence of γ-protonated GTP. The location of the protonated group is indicated (arrow). (b) Continuous measuring of RMSD (upper panel, color coded as in Fig. 1) and of C^{α}–C^{α} distances between residues E302–K205 and D26–K80 (blue and red lines, respectively; lower panel) during a 5 -ns MD trajectory simulating low pH conditions. (c) GTPase activity measured for purified $FtsZ_{EC}$ (left) and $FtsZ_{MJ}$ (right) at different pH values. To cover a wide range of pH values and to avoid buffer-specific effects, we used several buffers with overlapping pH ranges. Citrate phosphate buffers, providing the widest range of buffer capacity with constant ionic strength, were done as described by Stoll and Blanchard.[28]

range of pH values, from 4.8 to 8.0. Figure 3c summarizes the results. In agreement with the MD prediction, values of GTPase activity for both molecules significantly decrease when pH changes from 7.0 to 6.0 and become undetectable at pH values lower than 5.5. The putative denaturalization of FtsZ at these pH values was discarded, as it has been reported that $FtsZ_{EC}$ structure denaturalization occurs only at pH values around 3.0,[29] being the protein completely structured at pH 6.0.[30] The experiment was also done at pH values of up to 8.0, although these conditions cannot be simulated in the MD environment, as all Arg and Lys residues were already completely protonated at neutral pH in the simulation. The behaviors of $FtsZ_{MJ}$ and $FtsZ_{EC}$ were similar at all measured pH values, exhibiting the GTPase activity of $FtsZ_{MJ}$ to be of higher variability at pH values in the range 6.5–8.0 as compared with that of $FtsZ_{EC}$. Finally, to analyze the capacity of FtsZ to polymerize in the absence of GTPase activity at acidic pH values, we performed a series of light-scattering experiments using $FtsZ_{EC}$ and $FtsZ_{MJ}$. In accordance with the profiles for GTPase activity at low pH values, both proteins showed increasing maximum signal values and maintained them for long periods (up to 10 min at pH 6.0) when the experiments were performed at lower pH values (Fig. 4a). To ensure that the same polymers were obtained at different pH values, we analyzed aliquots of different extracts by electron microscopy. The results shown in Fig. 4b ($FtsZ_{EC}$) and c ($FtsZ_{MJ}$) indicate the presence of polymers at all pH values. At lower pH values, there was a trend to form filament bundles that gave higher light-scattering signal and could be detected by electron microscopy. Filament bundling has been described

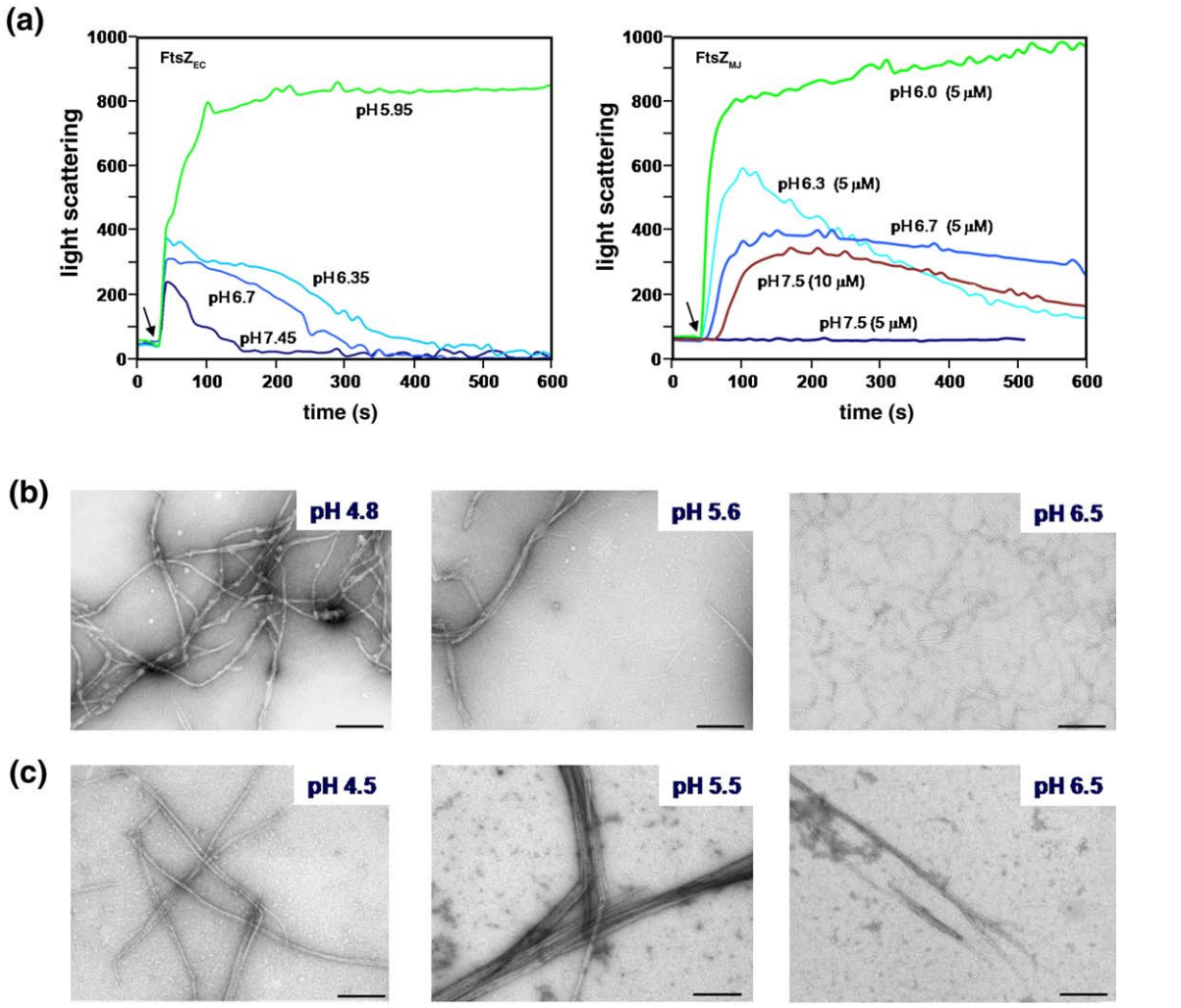

Fig. 4. Polymerization of FtsZ at low pH. (a) Light-scattering analysis of the assembly of purified $FtsZ_{EC}$ at 10 μM (left) and $FtsZ_{MJ}$ at 5 or 10 μM (right). Polymerization in citrate phosphate buffers at the indicated pH values was followed by 90° light scattering as indicated in Fig. 2. The arrow indicates the point at which GTP (final concentration of 0.5 mM) was added. (b) Electron microscopy photographs of $FtsZ_{EC}$ at acidic pH values. Electron microscopy was performed as described previously.[13] FtsZ was incubated in 100 μl of polymerization buffer. GTP was added to 0.5 mM, and after 1 min, the samples were applied to 400-mesh collodion-coated, glow-discharged grids, negatively stained with 2% uranyl acetate, and inspected with a Jeol 1200EXII electron microscope. Bar represents 0.25 μm. (c) Electron microscopy photographs of $FtsZ_{MJ}$ (lower panel) at acidic pH values. Experimental conditions are as in (b).

before and is related to the formation of stable filaments with low GTPase activities.[13,30] This is in agreement with the model predicted by MD—at lower pH values, the dimer interface is more stable and the GTPase activity is lower, and these might favor the filament bundling.

In conclusion, the analysis of the behavior of FtsZ by MD simulation and by measuring GTPase activity and polymerization revealed an important role for potassium ions in positioning a catalytic water molecule in the active GTPase site and thus maintaining appropriate contact between residues at the dimer interface. Furthermore, it has been shown that GTPase activity depends on the protonation state of the gamma-phosphate of GTP, which offers a molecular explanation for the capacity of FtsZ to form stable polymers at low pH values, in the complete absence of GTPase activity.

Finally, an MD model for the preference of $FtsZ_{MJ}$ for K^+ over Na^+ as the monovalent ion and for the inhibitory role of Na^+ in the active center of the protein has been offered. This model can be extended to other enzymes complexed to monovalent cations.[21,22]

Acknowledgements

This study was supported by the Spanish Ministerio de Educación y Ciencia through grants SAF2007-61926 (to P.G.-P.) and BIO2005-02194 (to M.V.); by CIBER Fisiopatología de la Obesidad y Nutrición, an initiative of Instituto de Salud Carlos III (to P.G.-P.); by the Comunidad de Madrid through grant S-BIO-0260/2006-COMBACT (to P. G-P., J. Mingorance, and M.V.); and by the European Union through grant FP7-223431 (EU "Divinocell" project; to P.G.-P. and M.V.). Financial support from the "Fundación Ramón Areces" to CBMSO is also acknowledged. J. Mingorance was a recipient of a Ramón y Cajal fellowship financed by the European Social Fund and the Ministerio de Educación y Ciencia. A.I.R. was a recipient of an I3P contract from the Spanish Council for Scientific Research. We also thank "Centro de Cálculo Científico" (CCC-UAM) for computational support. Work at Biomol-Informatics SL was partially financed by the European Social Fund.

References

1. Rueda, S., Vicente, M. & Mingorance, J. (2003). Concentration and assembly of the division ring proteins FtsZ, FtsA, and ZipA during the *Escherichia coli* cell cycle. *J. Bacteriol.* **185**, 3344–3351.
2. Vicente, M. & Rico, A. I. (2006). The order of the ring: assembly of *Escherichia coli* cell division components. *Mol. Microbiol.* **61**, 5–8.
3. Erickson, H. P. (2007). Evolution of the cytoskeleton. *BioEssays*, **29**, 668–677.
4. López-Viñas, E. & Gómez-Puertas, P. (2004). Sequence and structural alignments of eukaryotic and prokaryotic cytoskeletal proteins. In *Molecules in Time and Space: Bacterial Shape, Division and Phylogeny* (Vicente, M., Tamames, J., Valencia, A. & Mingorance, J., eds), pp. 155–172, Kluwer Academic/Plenum Publishers, New York, NY.
5. Mingorance, J., Rico, A. I. & Gómez-Puertas, P. (2004). Bacterial morphogenes. In *Molecules in Time and Space: Bacterial Shape, Division and Phylogeny* (Vicente, M., Tamames, J., Valencia, A. & Mingorance, J., eds), pp. 173–194, Kluwer Academic/Plenum Publishers, New York, NY.
6. Lutkenhaus, J. (2007). Assembly dynamics of the bacterial MinCDE system and spatial regulation of the Z ring. *Annu. Rev. Biochem.* **76**, 539–562.
7. Li, Z., Trimble, M. J., Brun, Y. V. & Jensen, G. J. (2007). The structure of FtsZ filaments *in vivo* suggests a force-generating role in cell division. *EMBO J.* **26**, 4694–4708.
8. Mingorance, J., Tadros, M., Vicente, M., Gonzalez, J. M., Rivas, G. & Velez, M. (2005). Visualization of single *Escherichia coli* FtsZ filament dynamics with atomic force microscopy. *J. Biol. Chem.* **280**, 20909–20914.
9. Osawa, M., Anderson, D. E. & Erickson, H. P. (2008). Reconstitution of contractile FtsZ rings in liposomes. *Science*, **320**, 792–794.
10. Horger, I., Velasco, E., Mingorance, J., Rivas, G., Tarazona, P. & Velez, M. (2008). Langevin computer simulations of bacterial protein filaments and the force-generating mechanism during cell division. *Phys. Rev. E: Stat. Nonlin. Soft Matter Phys.* **77**, 011902.1–011902.9.
11. Horger, I., Velasco, E., Rivas, G., Velez, M. & Tarazona, P. (2008). FtsZ bacterial cytoskeletal polymers on curved surfaces: the importance of lateral interactions. *Biophys. J.* **94**, L81–L83.
12. Surovtsev, I. V., Morgan, J. J. & Lindahl, P. A. (2008). Kinetic modeling of the assembly, dynamic steady state, and contraction of the FtsZ ring in prokaryotic cytokinesis. *PLoS Comput. Biol.* **4**, e1000102.
13. Mingorance, J., Rueda, S., Gomez-Puertas, P., Valencia, A. & Vicente, M. (2001). *Escherichia coli* FtsZ polymers contain mostly GTP and have a high nucleotide turnover. *Mol. Microbiol.* **41**, 83–91.
14. Mukherjee, A. & Lutkenhaus, J. (1999). Analysis of FtsZ assembly by light scattering and determination of the role of divalent metal cations. *J. Bacteriol.* **181**, 823–832.
15. Sossong, T. M., Jr, Brigham-Burke, M. R., Hensley, P. & Pearce, K. H., Jr. (1999). Self-activation of guanosine triphosphatase activity by oligomerization of the bacterial cell division protein FtsZ. *Biochemistry*, **38**, 14843–14850.
16. Tadros, M., Gonzalez, J. M., Rivas, G., Vicente, M. & Mingorance, J. (2006). Activation of the *Escherichia coli* cell division protein FtsZ by a low-affinity interaction with monovalent cations. *FEBS Lett.* **580**, 4941–4946.
17. Rivas, G., Lopez, A., Mingorance, J., Ferrandiz, M. J., Zorrilla, S., Minton, A. P. *et al.* (2000). Magnesium-induced linear self-association of the FtsZ bacterial cell division protein monomer. The primary steps for FtsZ assembly. *J. Biol. Chem.* **275**, 11740–11749.
18. Lu, C., Stricker, J. & Erickson, H. P. (1998). FtsZ from *Escherichia coli*, *Azotobacter vinelandii*, and *Thermotoga maritima*—quantitation, GTP hydrolysis, and assembly. *Cell Motil. Cytoskeleton*, **40**, 71–86.
19. Oliva, M. A., Huecas, S., Palacios, J. M., Martin-Benito, J., Valpuesta, J. M. & Andreu, J. M. (2003). Assembly of

archaeal cell division protein FtsZ and a GTPase-inactive mutant into double-stranded filaments. *J. Biol. Chem.* **278**, 33562–33570.
20. Suelter, C. H. (1970). Enzymes activated by monovalent cations. *Science*, **168**, 789–795.
21. Page, M. J. & Di Cera, E. (2006). Role of Na^+ and K^+ in enzyme function. *Physiol. Rev.* **86**, 1049–1092.
22. Di Cera, E. (2006). A structural perspective on enzymes activated by monovalent cations. *J. Biol. Chem.* **281**, 1305–1308.
23. Oliva, M. A., Cordell, S. C. & Lowe, J. (2004). Structural insights into FtsZ protofilament formation. *Nat. Struct. Mol. Biol.* **11**, 1243–1250.
24. Case, D. A., Cheatham, T. E., III, Darden, T., Gohlke, H., Luo, R., Merz, K. M., Jr *et al.* (2005). The Amber biomolecular simulation programs. *J. Comput. Chem.* **26**, 1668–1688.
25. Diaz, J. F., Kralicek, A., Mingorance, J., Palacios, J. M., Vicente, M. & Andreu, J. M. (2001). Activation of cell division protein FtsZ. Control of switch loop T3 conformation by the nucleotide gamma-phosphate. *J. Biol. Chem.* **276**, 17307–17315.
26. Hoenig, M., Lee, R. J. & Ferguson, D. C. (1989). A microtiter plate assay for inorganic phosphate. *J. Biochem. Biophys. Methods*, **19**, 249–251.
27. Kaczmarek, P., Szczepanik, W. & Jezowska-Bojczuk, M. (2005). Acid-base, coordination and oxidative properties of systems containing ATP, L-histidine and Ni(II) ions. *Dalton Trans.* **22**, 3653–3657.
28. Stoll, V. S. & Blanchard, J. S. (1990). Buffers: principles and practice. *Methods Enzymol.* **182**, 24–38.
29. Santra, M. K. & Panda, D. (2007). Acid-induced loss of functional properties of bacterial cell division protein FtsZ: evidence for an alternative conformation at acidic pH. *Proteins*, **67**, 177–188.
30. Beuria, T. K., Shah, J. H., Santra, M. K., Kumar, V. & Panda, D. (2006). Effects of pH and ionic strength on the assembly and bundling of FtsZ protofilaments: a possible role of electrostatic interactions in the bundling of protofilaments. *Int. J. Biol. Macromol.* **40**, 30–39.